Dual-stream jet noise test with internal mixer design variations for LTO noise of supersonic aircraft

Remco Habing, Mark-Jan van der Meulen, Maxime Huet, Robert Jaron, Francesco Petrosino, Mattia Barbarino, Oleksandr Zaporozhets

DUAL-STREAM JET NOISE TEST WITH INTERNAL MIXER DESIGN VARIATIONS FOR LTO NOISE OF SUPERSONIC AIRCRAFT

Remco Habing[1], Mark-Jan van der Meulen[1], Maxime Huet[2], Robert Jaron[3], Francesco Petrosino[4], Mattia Barbarino[4] & Oleksandr Zaporozhets[5]

[1]NLR – Netherlands Aerospace Centre, 8316 PR Marknesse, The Netherlands
[2]ONERA / DAAA, Université Paris Saclay, F-92322 Châtillon, France
[3]DLR – German Aerospace Center, 10625 Berlin, Germany
[4]CIRA – Italian Aerospace Research Centre, 81043, Capua (CE), Italy
[5]Institute of Aviation, 02-436 Warszawa, Poland

Abstract

One of the challenges of designing future commercial supersonic aircraft is accurate prediction and reduction of landing and takeoff (LTO) noise. It is expected that jet noise is a dominant noise source during LTO. In the present study a small-scale acoustic jet noise test has been designed and performed. The model contains a dual-stream nozzle including an external plug and has a modular design to vary nozzle length and internal mixers designs. An acoustic test in an anechoic environment with a sideline microphone array has been performed for a range of nozzle pressure ratios. The effect of mixer and lobes and nozzle length on the jet noise characteristics has been evaluated. Finally, a comparison with semi-empirical predictions for fully mixed flows shows the need for fast prediction of internally mixed exhaust systems.

Keywords: Jet noise, Internal mixer, External plug, Acoustic measurements

1. Introduction

Over the past decade, there has been a revival in publicly and privately funded development of civil supersonic aircraft, driven by increasing globalization and the associated need for shorter travel times. In the short term, the challenge for a successful market entry will be the landing and takeoff (LTO) noise as well as the significantly increased fuel consumption compared to conventional subsonic aircraft. In view of the need to reduce CO_2 emissions some manufacturers are investigating the use of sustainable aviation fuels. In the long term, new technologies are needed to reduce the sonic boom. Since the impact of sonic booms on living beings and building structures is generally unacceptable, supersonic flight over land is prohibited. As a result, the time advantage of supersonic aircraft would be limited mainly to routes with a large proportion over water.

With some manufacturers being already at an advanced stage of development, there is an urgent need for development of certainty with regard to noise and emissions standards. The state today for the certification rules of supersonic aircraft can be described as follows: whereas the noise standard (provided in Chapter 14 of ICAO Annex 16 Vol I) and the emission standard (to be found in Chapter 2 of ICAO Annex 16 Vol II) for subsonic aircraft have evolved over time as technologies have improved, there was not any development for supersonic aircraft at all. The noise and emission regulations in Chapter 12 of ICAO Annex 16 Vol I and Chapter 3 of ICAO Annex 16 Vol II, respectively, were originally created for the Concorde airplane and have remained unchanged ever since. Today, the noise standard is no longer valid, as it was limited in time, but the outdated emission standard is still applicable. Consequently, the International Civil Aviation Organization (ICAO) is required to establish updated standards for the possible launch of this new generation of commercial supersonic aircraft.

Since there are no available data of state-of-the-art commercial supersonic aircraft for determining new certification limits, the EU-Project SENECA (2021-2024, https://seneca-project.eu) aims at

supporting the certification authorities by providing those data. For that purpose, four different SST aircraft platforms ranging from supersonic business jets designed for cruise Mach numbers of Ma=1.4 and Ma=1.6 up to large airliners designed for 100 passengers and cruise Mach numbers of Ma=1.8 and Ma=2.2 are virtually designed in SENECA. Assessment of the prediction quality of LTO noise, especially that of jet noise which is believed to be the dominant noise source for commercial supersonic aircraft, is an important factor when providing noise data. Recent publications show early results of jet noise benchmarking activities conducted within the SENECA project [1,2].

In general, the choice of a nozzle to use on an aircraft engine exhaust system is determined by many factors, including noise produced by the exhaust flow. For supersonic transport aircraft, installed cruise performance and the ability to vary both throat and exit areas is a key factor. At cruise, the nozzle must be convergent-divergent to maximize nozzle thrust efficiency. However, during LTO operations, a divergent nozzle has separation which produces excess noise. Reducing effective boattail angle is important in mitigating sonic boom and reducing installed drag. Nozzles with a translating external plug offer the ability to change nozzle areas with a single-degree-of-freedom actuator and reduce the nacelle drag (compared to an internal plug) by reducing the angle from the point of maximum nacelle diameter to the nozzle exit. These factors are well understood [3]. It is less clear how these geometric features change the noise of the jet plume from that of a simple nozzle without an external plug. The acoustic differences are important because most prediction methods for jet noise of plug-based nozzles are based on simple internal plug nozzles, see e.g. Ref. [4,5,6].

A plug nozzle has certain advantages and offers an alternative to a convergent-divergent (CD) nozzle for application to supersonic aircraft concepts, see e.g. Table 1. For a literature review on the history and the pros and cons of plug nozzles the reader is referred to Ref. [7].

Table 1 – Pros and cons of external plug nozzle vs. CD nozzle.

	External plug nozzle	CD nozzle
Pros	- possible shock noise reduction during LTO - reduced hardware complexity - maintain thrust at off-design condition - reduced design complexity	- max. thrust efficiency at cruise - lower weight - no cooling
Cons	- added weight - heat transfer issues (cooling) - reduced performance for external flow (large boattail drag)	- thrust loss at low altitude - design complexity - hardware complexity

In internally mixed exhaust systems, the two streams of air meet at the trailing edge of a splitter, which is often lobe-shaped to promote rapid mixing of the two streams. This ‘forced mixer’ is the object of optimization efforts because the transference of thermal energy between the two streams by mixing within the duct can produce some thrust increase to the system [3]. Factors such as pressure losses, friction losses, mechanical weight, dimensional stability and durability are also critical in the design of these mixers [3]. From the perspective of fluid mechanics, the better the mixing, the closer the flow at the exit of the nozzle is to a single-stream jet. Commercial supersonic aircraft will require exhaust nozzle systems that are nearly as quiet as conventional aircraft systems while offering high aerodynamic performance. The internally mixed, external plug nozzle exhaust system appears as a promising candidate for such aircraft. However, the noise of such systems has been only poorly understood and, recalling Ref. [3], “no studies of the noise from internally mixed exhaust systems with external plugs was found in the literature” until 2021. Since then physics-based simulations are performed to generate relevant data for prediction of uncertainty reduction [16]. Typical mixer designs contain following parameters: lobe count, penetration, lobe bias, mixer length, trailing edge (TE) slope and more advanced features might contain scalloped lobes, cutbacks on TE, lobe vents, vortex generators and TE chevrons [16]. In 2021 the work of Bridges and Wernet [3] addresses two questions: i) how do external plugs and internal mixers separately affect the far-field noise, and ii) what are their interdependent effects? The focus was on broadband shock noise

effects. Driven by the certification constraint in the SENECA project, the present study aims to explore the jet noise characteristics for high-subsonic conventional profile dual-stream flows, limited to test facility cold flows, considering only a single external plug with focus on the effect of some internal mixer / nozzle configurations.

2. Model design and manufacturing

In order to obtain a test model being representative to future commercial supersonic aircraft, the following exhaust nozzle designs have been taken as starting point from the NASA Plug20 test report [8]: 122DLm5p2079 (external plug, internal mixer, nozzle duct parts, plug base / extension and internal plug tip). The geometry was provided as STEP files.

Then the mixer geometry has been parameterized in CAD to allow number of lobes variations and to smoothen the geometry. The model is a modular design in which various configurations such as different mixers, nozzle lengths and a coannular nozzle can be tested. The model size for small-scale testing was determined by the following constraints:

- Mass-flow constraint of pressurized air system
- Acoustic true far-field constraint

For the first constraint the nozzle exit area is scaled down to yield the maximum mass-flow rate (ca. 1.0 kg/s) at a slightly supersonic jet condition. For the second constraint the nozzle exit dimensions are scaled down to yield a minimum required microphone position [9,10] still mountable in the anechoic room available space. It appeared that the overall constraint is dominated by the mass-flow requirement.

After having defined the scaling factor (equal to 2.9 w.r.t. Plug20), the nozzle model parts were scaled and new interfacing structures (convergent ducts) were designed for application in NLR's AWT facility with an available pressurized air supply system [11]. In addition, additional parts have been designed and realized, i.e. a coannular nozzle outer duct (for internal plug), 18 nozzle surface static pressure taps, and 2 x 2 resonance breaking tabs at the nozzle exit. Figure 1 - Figure 3 show the model key designs.

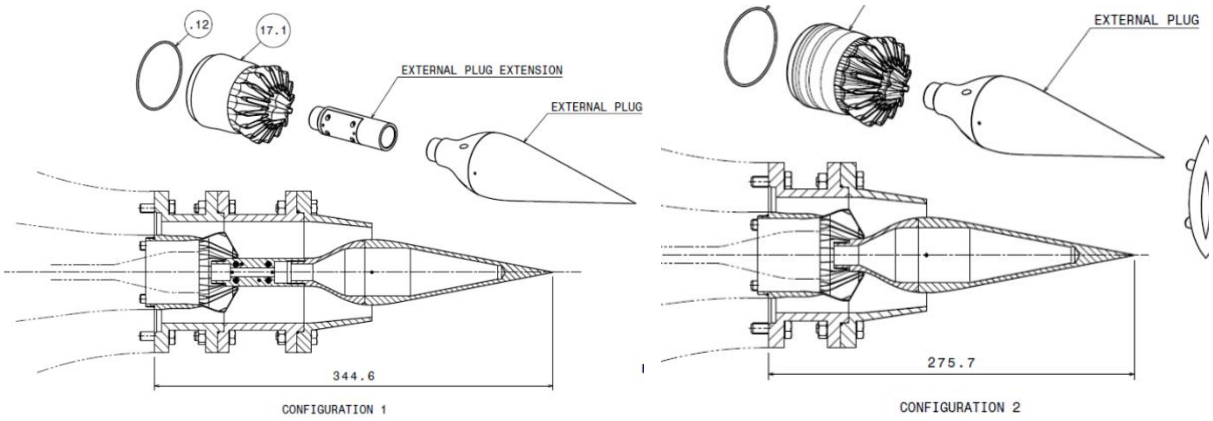

Figure 1 – Design of small-scale nozzle model parts: mixer with 16 lobes, (left) long duct, (right) short duct.

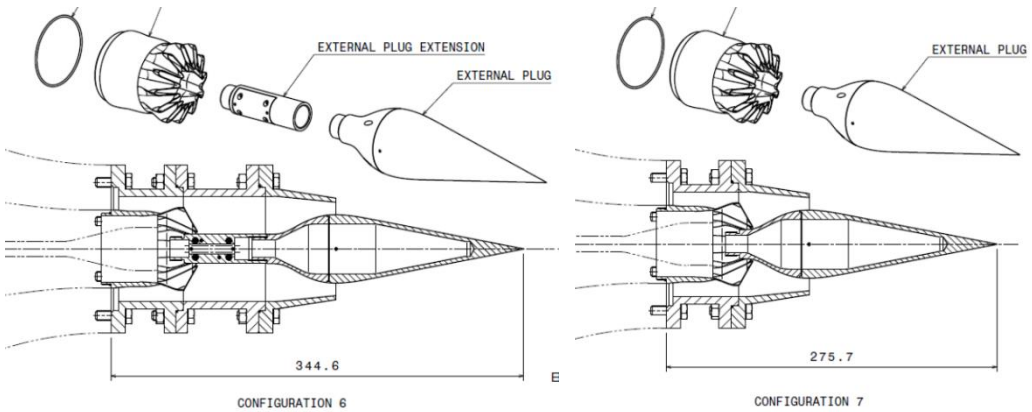

Figure 2 – Design of small-scale nozzle model parts: mixer with 12 lobes, (left) long duct, (right) short duct.

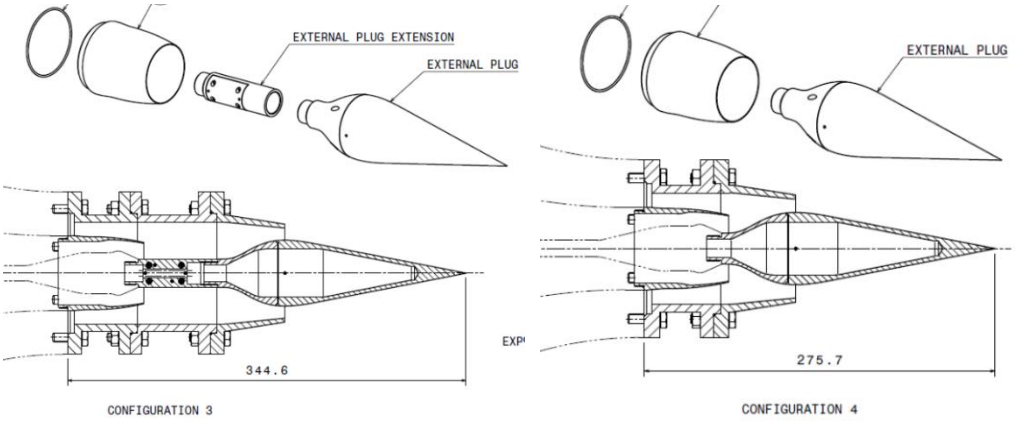

Figure 3 – Design of small-scale nozzle model parts: without lobed mixer, (left) long duct, (right) short duct.

Most structures have been milled out of aluminum, but the internal mixer parts have been 3D metal printed. Figure 4 illustrates some manufactured nozzle parts.

Figure 4 – Example of manufactured nozzle parts in partially dismounted state.

3. Test and measurement setup

3.1 Pressurized air system

In order to generate a dual-stream jet in the model nozzle, an external air supply system was rented. This system features a compressor, adsorption dryer and split piping with individual pressure regulators for the dual streams. The upstream part of the modular nozzle interface is connected to the dedicated supply unit, see left hand side of Figure 5. The inner (core) duct has an axial flange for the pressurized air tube and includes metal foam plates, a total pressure and total temperature sensor in a settling environment and turbulence screens to improve the flow quality before air being accelerated into the nozzle part. The annular outer (bypass) duct has two radial flanges for the pressurized air tubes and also includes metal foam disks to homogenize the dual radial incoming flow and enable supply line spurious noise damping and turbulence screens. The outer duct is also instrumented with a total pressure and total temperature sensor. The metal foam plates are used to enable sound absorption of possible supply line noise and nozzle reflected noise (preventing standing waves).The core duct is fixed to the outer duct upstream of the turbulence screens by three NACA0010 profile shaped struts.

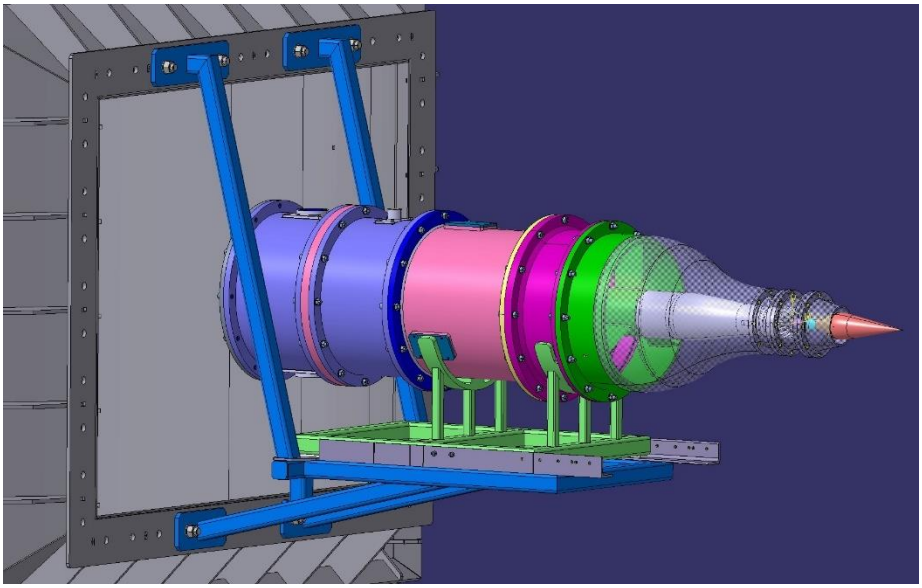

Figure 5 – Design of dual stream pressurized air supply unit.

3.2 Acoustic measurement set-up

The experiment has been performed in NLR's Aero-acoustic Wind Tunnel (AWT). Rather than using a closed- or open test section, the jet noise test-setup was conducted without operating wind tunnel flow. The anechoic chamber has a volume of 8m x 9m x 5m, with a specified sound absorption coefficient of 99% for frequencies above 200 Hz. The dedicated supply unit was mounted on the tunnel contraction structure. The tunnel collector was used to capture the expanded jet flow. A ventilation hatch in the AWT circuit was opened for venting and the contraction of the AWT was closed to prevent circulation. The dual stream nozzle jet Mach numbers can be controlled individually by using two remote controlled pressure regulators for the air supply lines. The jet Mach number can be derived by measuring the supply total pressure, ambient and nozzle surface static pressures and applying isentropic flow relations. However, in order to allow comparison between different nozzle configurations, the nozzle pressure ratio NPR (i.e. stagnation pressure divided by ambient static pressure) has been set for each stream and each test condition.

In order to measure the acoustic far-field, a minimum distance from noise source to the microphone positions is required. This minimum depends on the type of jet (i.e. subsonic, supersonic cold, supersonic heated and single versus dual-stream jet) [9,10]. The present test set-up only allows cold/unheated jet testing where the geometry based far-field requirements are met. The nozzle suspension can be traversed in flow direction to keep the nozzle exit plane fixed in space for all nozzle configurations. However, for the present test the nozzle exit position is not fixed and the directivity angles are updated according to the nozzle configuration. The microphone array consists of 11 ¼" free-field microphones that are mounted on fixed poles and set at normal incidence to the nozzle exit. The vertical and horizontal support rods are acoustically treated. The microphones are placed at equidistant polar angles of 10 deg in the range of 50 – 150 deg (long nozzle), see Figure 6. In order to allow data processing with atmospheric damping correction, the ambient conditions (i.e. static pressure, static temperature and relative humidity) are also measured.

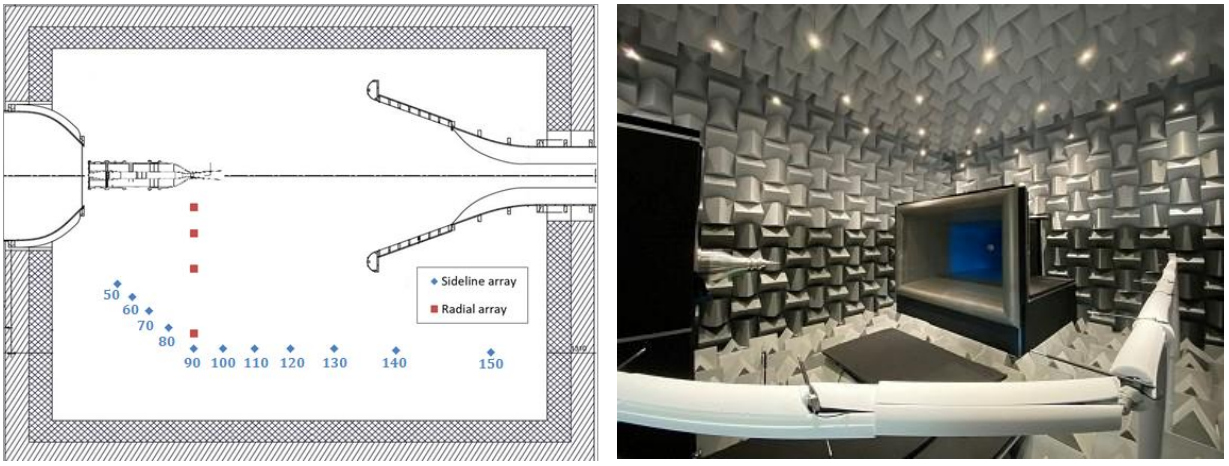

Figure 6 – Microphone array in NLR-AWT anechoic room: (left) sketch of directivities, (right) picture.

The protective grids of the microphones are removed to prevent internal resonances / scattering and the factory frequency response fit curves are implemented to yield a flat response up to 100 kHz. In order to allow for anechoic checks, additional microphones are installed at various lateral positions. The acoustic data is acquired by a 16 bit multi-channel dynamic data acquisition system (with sampling frequency = 200 kHz/channel, measurement time = 30 s, auto-ranging, HPF = 1.5 Hz). The data post-processing included microphone sensitivity correction, atmospheric absorption correction and geometric spreading correction to yield SPL spectra at a reference distance.

3.3 Test program

Prior to the test program, various checks have been performed. These include: pre-assembly nozzle parts, background noise measurements, check signal-to-noise ratio, controllability at low NPR, maximum attainable NPR, check and reduce possible resonances, check nozzle static pressure distribution, repeatability checks. The test program contained the following format for each nozzle configuration:

- Background noise (inner and outer: NPR = 1)
- Equivalent single stream (inner and outer: NPR = 1.1 - 1.9)
- Hot core simulation (outer NPR = 1.1, inner NPR = 1.2 - 2.1)

For the coannular (internal plug) nozzle also single stream conditions have been measured. Table 2 shows the nozzle configurations that have been tested. Experience with dual-stream jet noise testing showed that ring-resonances at an annular nozzle exit could occur [11]. As risk-mitigation for possible suppression of those kind of resonances, dedicated tabs and related dummy inserts for the inner- and outer duct have been designed and manufactured.

Table 2 – Performed test matrix.

RUN	Configuration			
	External plug	Lobed mixer	Nozzle length	Tabs
1	yes	yes (16 lobes)	long	no
2	no	no	coannular plug	no
3	yes	no	long	no
4	yes	no	long	yes
5	yes	no	short	yes
6	yes	yes (16 lobes)	short	yes
7	yes	yes (16 lobes)	long	yes
8	yes	yes (12 lobes)	long	yes
9	yes	yes (12 lobes)	short	yes
10	yes	yes (16 lobes)	long	no

4. Experimental results

4.1 Data quality evaluation

With the radial acoustic array, anechoic conditions can be evaluated. The anechoic room is designed to absorb the noise generated by a source, thereby avoiding reflections and acoustic interference. If this is the case, the sound pressure amplitude should decrease inversely proportional with distance between the source and the microphone head. Additionally, acoustic energy is absorbed by the medium in which the acoustic waves travel. For the typical audible frequency range this is a negligible effect within the dimensions of the anechoic room. However, for higher frequencies (due to model scale) this can have a significant effect and should be taken into account in the evaluation of the anechoic properties of the room. The data is corrected for geometric spreading (to a reference distance equal to the 90 deg sideline microphone head) and atmospheric damping according to ISO 9613. Figure 7 shows an example where the dashed lines are uncorrected spectra and the solid lines are corrected spectra. The corrected SPL spectra collapse well (< 1 dB), showing proper anechoic conditions in the third-octave band frequency range [315 Hz, 80 kHz].

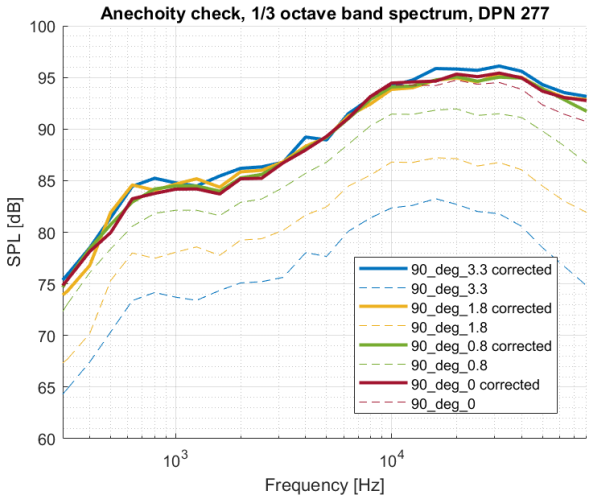

Figure 7 – Anechoity check.

During the test several short-term and long-term repeat points were recorded. A typical repeatability of 1 dB up to 80 kHz was found for the broadband jet noise spectra, see Figure 8 (left) as example. The primary use of applying tabs was to suppress ring-resonances. However, tabs could also affect the broadband noise levels. Figure 8 (right) shows that the effect of tabs is not significantly affecting the narrowband spectra in the full range. Finally, it is noted that comparison of jet noise spectra with background noise spectra reveal sufficient signal-to-noise ratio in the full frequency range.

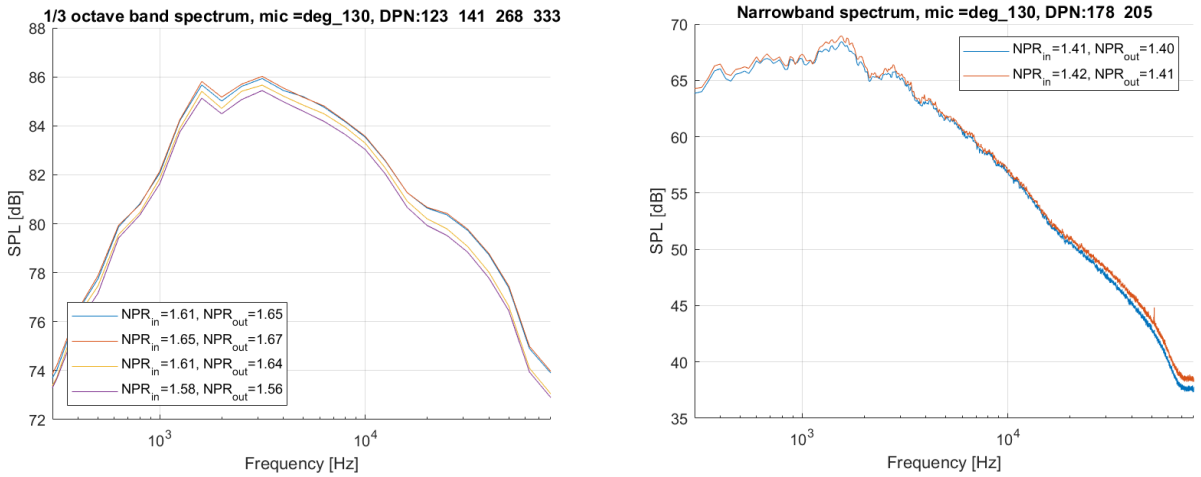

Figure 8 – Repeatability check (left) and Effect of tabs (right).

4.2 Effect of mixer and lobes

In order to investigate the effect of a mixer, narrowband SPL spectra at 130 deg polar angle (selected for known strong directivity) were generated where each plot shows the curves for a nozzle configuration without mixer, with 12 lobed mixer and with 16 lobed mixer. As the nozzle length is also a parameter of investigation in the present study, these plots are shown in Figure 9 and Figure 10 for a short nozzle and long nozzle, respectively.

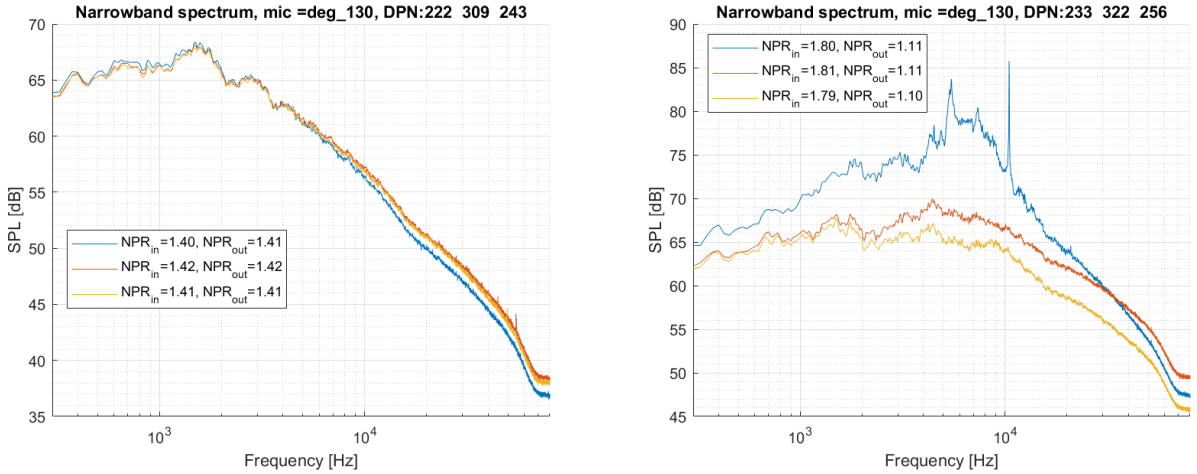

Figure 9 – Effect of mixer and lobes (blue = without mixer, red = 12 lobes, yellow = 16 lobes): short nozzle, (left) eq. single stream, (right) strong CP.

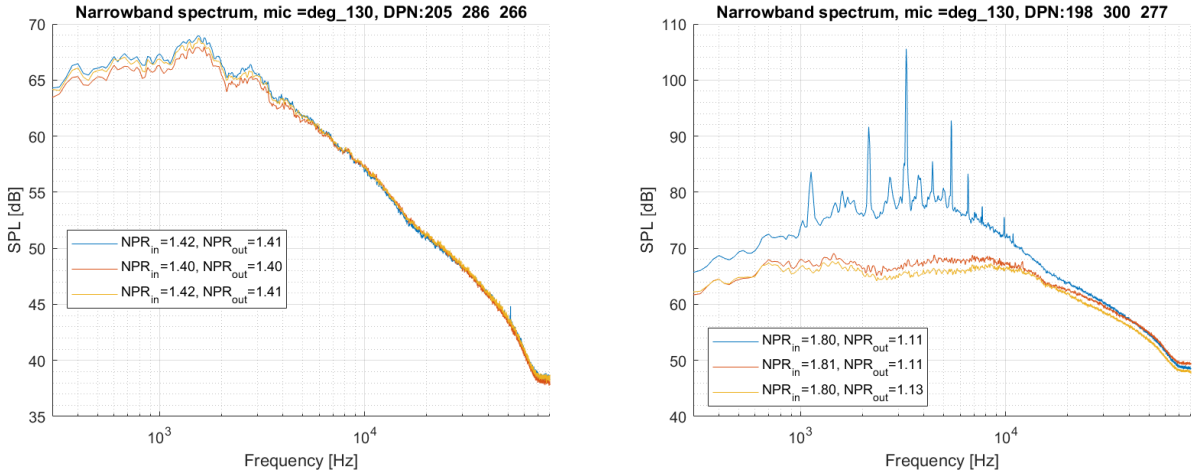

Figure 10 - Effect of mixer and lobes (blue = without mixer, red = 12 lobes, yellow = 16 lobes): long nozzle, (left) eq. single stream, (right) strong CP.

The right-handed figures represent a condition with strong conventional profile (CP) dual-stream flow. It is observed that for the configuration without mixer strong peaks are appearing in the spectra. The mechanism is currently not known to the authors. As for these configurations tabs have been applied, thus preventing ring resonances, the results might suggest that the peaks are laminar flow induced tones. Ad-hoc application of zig-zag tape to enforce turbulence transition was unsuccessful as the tape could not resist the flow. The spectra show that the mixers reduce broadband jet noise in a broad frequency range and suppress the peaks additionally. Increasing the number of lobes for a short nozzle can reduce the noise further in the middle and high frequency range. Furthermore, in case both streams have the same total pressure (and total temperature), the nozzle flow can be expected to be of type equivalent single stream, where a mixer cannot have a beneficial effect. The left-handed figures represent such a condition and show that for i) a long nozzle indeed no significant effect is occurring, but for ii) a short nozzle marginal high-frequency self-noise is generated.

Figure 11 shows the effect of a mixer on the directivity pattern. The directivity is calculated by i) correcting the third-octave band spectra for geometric spreading and atmospheric damping, and ii) energetic summation of all frequency bands. This results into the overall SPL at the selected

reference distance. It can be observed that a mixer changes the directivity characteristic for high emission angles, where the number of lobes is not affecting the directivity.

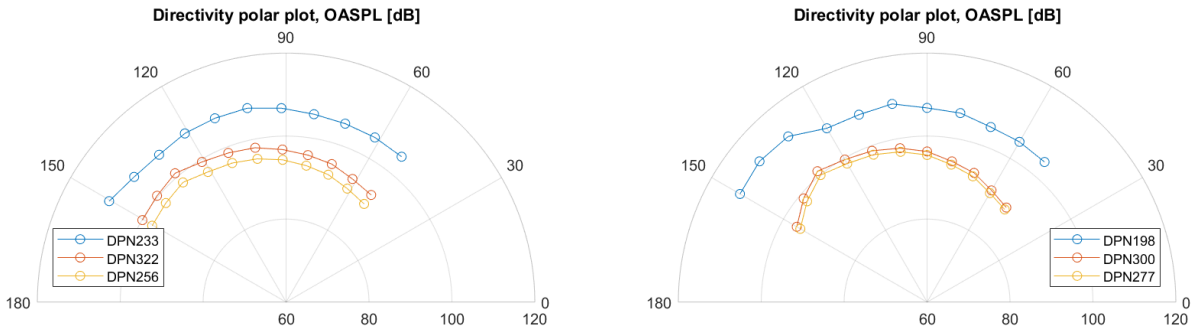

Figure 11 – Effect of mixer and lobes on directivity (blue = without mixer, red = 12 lobes, yellow = 16 lobes), (left) short nozzle, (right) long nozzle.

4.3 Effect of nozzle length

In order to investigate the effect of nozzle length, narrowband SPL spectra at 130 deg polar angle (selected for known strong directivity) were generated where each plot shows the curves for a short nozzle and a long nozzle. As the mixer is also a parameter of investigation in the present study, these plots are shown in Figure 12 and Figure 13 for a nozzle without mixer and with 16 lobes mixer, respectively.

The left-handed figures represent an equivalent single stream condition. The spectra show that no significant effect of nozzle length is present, as expected, where the small offset in NPR might be causing the small spectral difference for the configuration without mixer, which fully disappears for the mixed flow configuration.

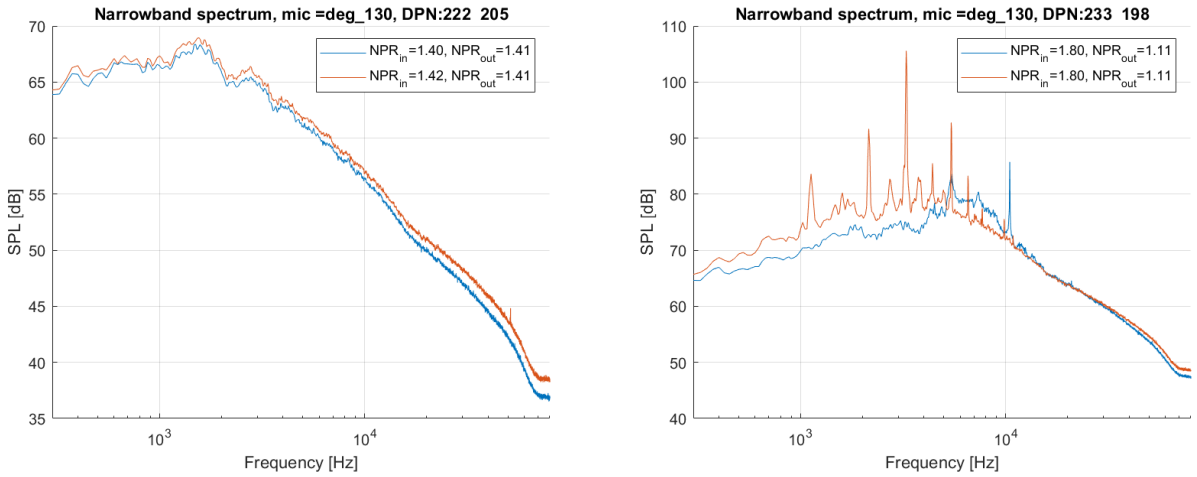

Figure 12 – Effect of nozzle length (blue = short, red = long): without mixer, (left) eq. single stream, (right) strong CP.

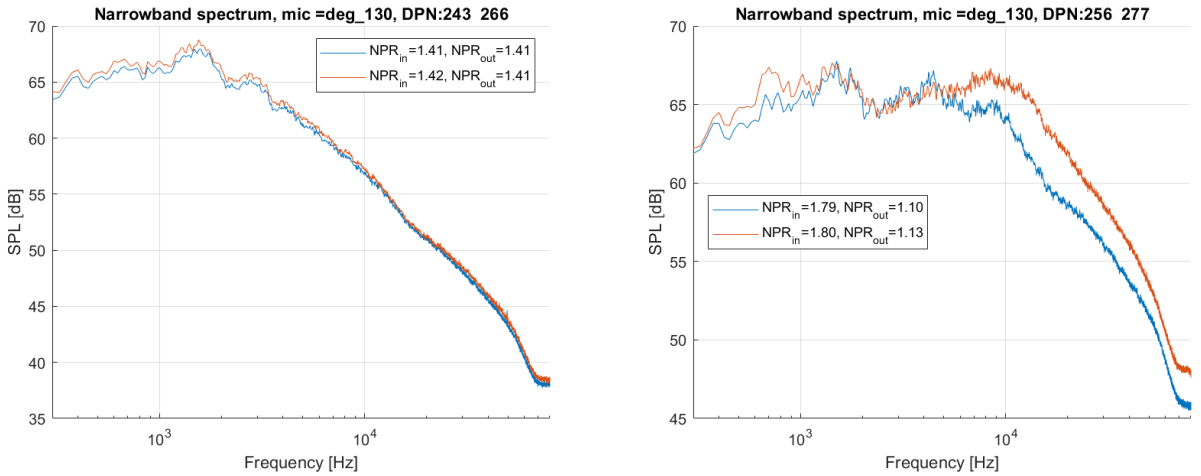

Figure 13 - Effect of nozzle length (blue = short, red = long): 16 lobes mixer, (left) eq. single stream, (right) strong CP.

The right-handed figures represent a condition with strong CP flow. Different effects for unmixed and mixed flow can be observed. Increasing the nozzle length for unmixed flows i) reduces the noise in the middle frequency range, ii) increases the noise in the low frequency range, and iii) can generate (laminar flow induced) tones in a broad frequency range. On the other hand, increasing the nozzle length for mixed flows can result into increased noise levels in the high frequency range.

Figure 14 shows the directivity polar plots for the condition with strong CP flow. For unmixed flows increasing the nozzle length changes the directivity only for the higher radiation angles (due to generation of strong tones). For mixed flows increasing the nozzle length amplifies the directivity pattern to a slightly increased maximum OASPL in the higher polar angle range.

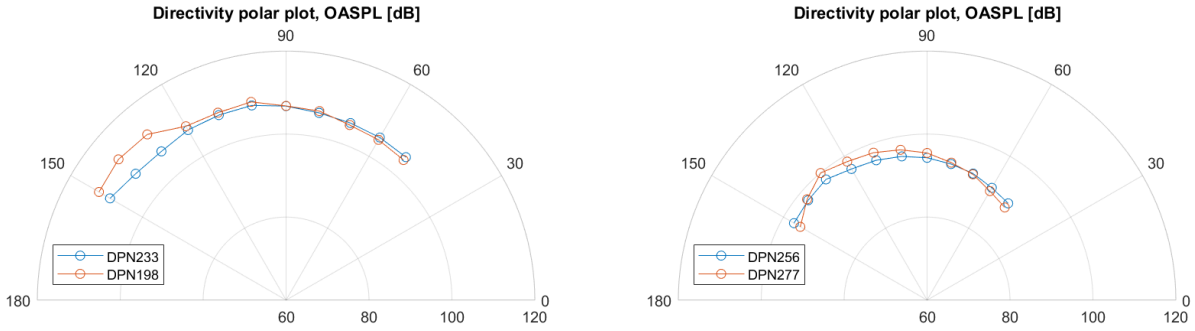

Figure 14 – Effect of nozzle length on directivity for strong CP flow (blue = short, red = long): without mixer (left), 16 lobes mixer (right)

5. Comparison with predictions

A database with processed experimental data has been generated and includes all configurations tested (Table 2). It consists of an acoustic part (third-octave band SPL spectra, OASPL, polar angle) and flow conditions part (covering all required input data for the used jet noise prediction methods [4,5,6], and static pressure distribution along nozzle surfaces).

The prediction tools have been evaluated in a benchmark assessment prior to the present study [1,2]. A comparison assessment of the third-octave band SPL spectra between experimental data and jet noise predictions with the Stone (2009) model [6] has been performed. This section presents such a comparison for a coannular nozzle first and then nozzles with external plug distinguishing effects of mixer and nozzle length. As the semi-empirical prediction models can be considered as low-fidelity, some high-fidelity simulation results will be evaluated additionally.

5.1 Coannular nozzle

Figure 15 shows the SPL spectra of the dedicated coannular plug nozzle with a subsonic conventional profile dual stream condition (NPR_{inner}=1.6, NPR_{outer}=1.1). The simulated spectrum contains a noise source breakdown and suggests that the found high-frequency bump in the experimental data can be explained by plug separation noise.

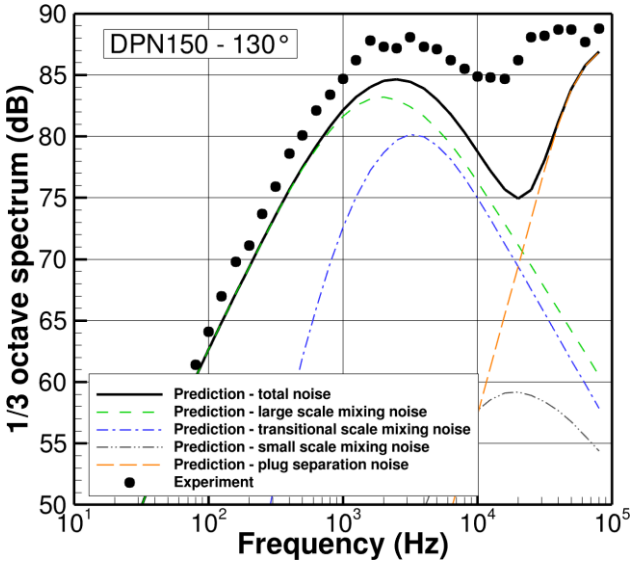

Figure 15 – Comparison between measured and predicted jet noise of a coannular nozzle, conventional-profile dual-stream.

Figure 16 shows this nozzle under a pure single stream condition (i.e. without outer stream), where the NPR_{inner} is set at a value of 2.0. The simulation has been performed with the conditions based on the measured static pressure slightly upstream of the nozzle exit, resulting in a subsonic jet. For high polar angles the high-frequency bump is still visible. In order to evaluate whether this could be the effect of shock noise, a low polar angle (i.e. forward radiation) result has been plotted as well. Figure 17 shows the simulated result with the assumption of the jet expanding under ambient static pressure. This adds a shock noise source (jet Mach nr. equal to 1.05), yielding improved agreement with the experimental data for both forward- and rearward radiation. The high-frequency bump as measured for this condition could thus only be partly explained by plug separation.

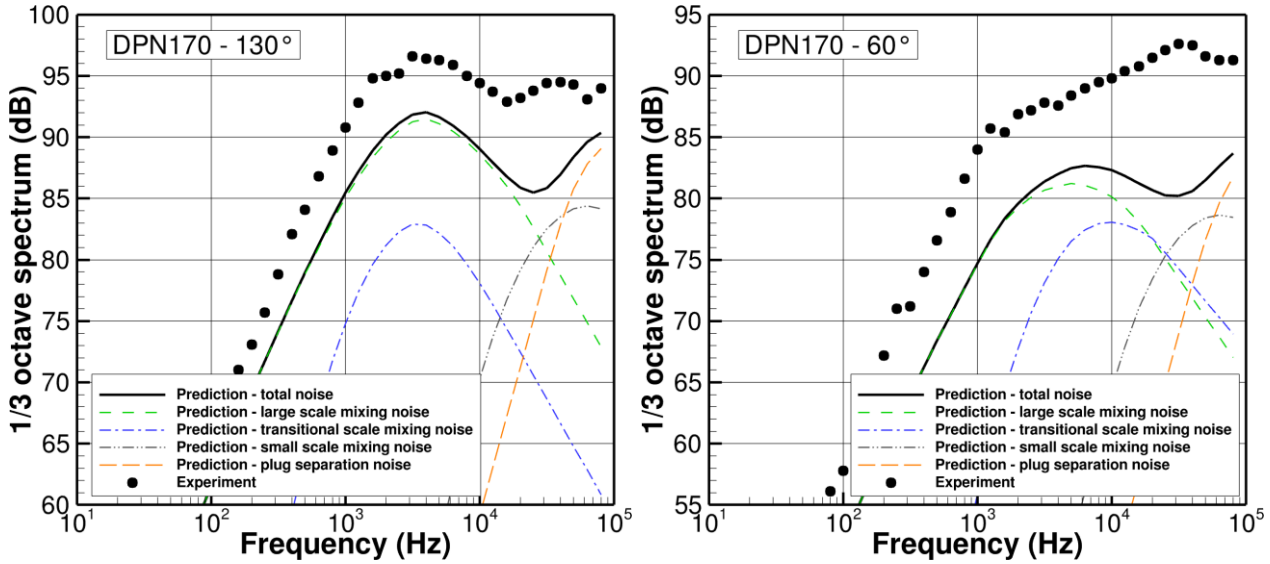

Figure 16 – Comparison between measured and predicted jet noise of a coannular nozzle with single stream plug at inner duct, (left) polar angle 130 deg, (right) polar angle 60 deg.

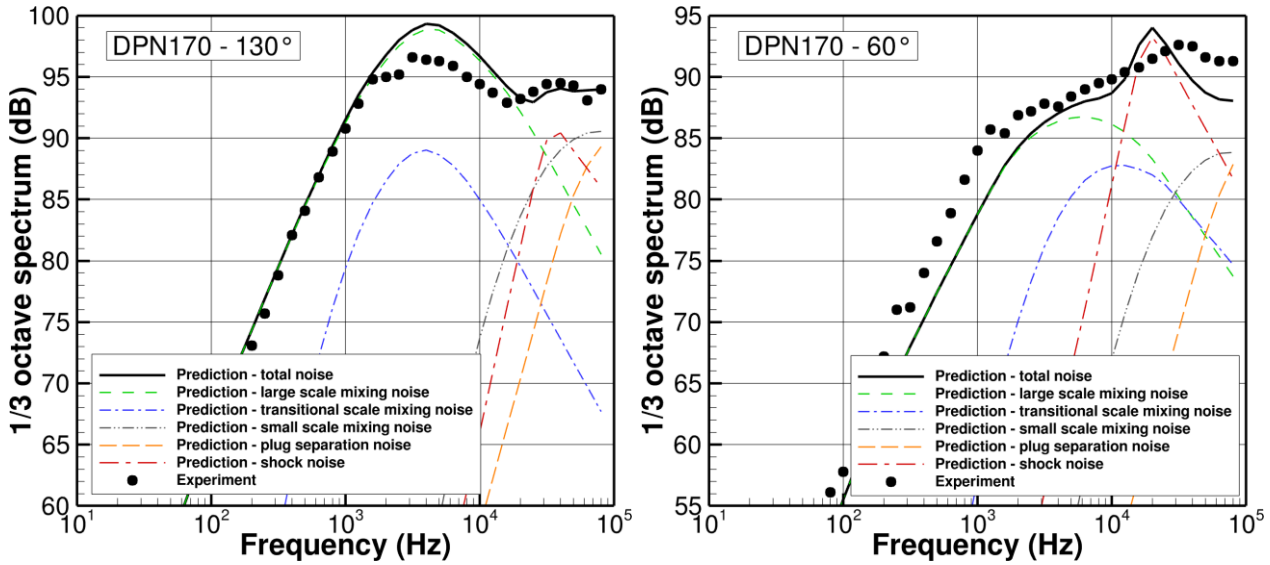

Figure 17 – Comparison between measured and predicted jet noise of a coannular nozzle with choked flow assumption of single stream plug at inner duct, (left) polar angle 130 deg, (right) polar angle 60 deg.

5.2 Effect of mixer

As there are no publicly available semi-empirical prediction methods for internally mixed exhaust flows, the following attempt was made to model the effect of a forced mixer. For mixed-flow nozzles (i.e. inner- and outer stream have different flow properties), the modelling has been performed by assuming a single stream jet with perfect mixing. This is done by applying conservation of mass and stagnation enthalpy and using the experimental data for mass-flow and stagnation temperature per stream duct.

Simulations have been performed for a long and short nozzle with external plug. Figure 18 shows a summary of the found experimental spectra for the configurations without mixer and mixer with 12 and 16 lobes, respectively. The simulated spectra are plotted as dashed lines. Although the simulations are underpredicting the mid-to-high frequency noise (due to perfect mixing), a similar qualitative trend for the mixer effect can be observed (resulting from changes in flow conditions).

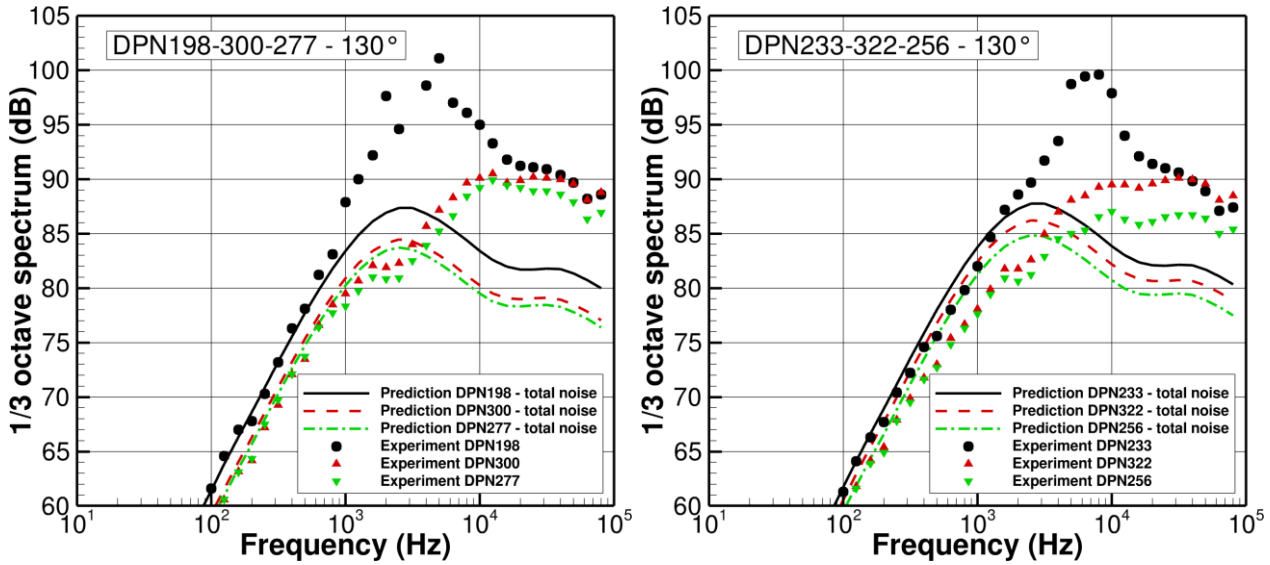

Figure 18 –Comparison between measured and predicted jet noise: effect of mixer for (left) long nozzle and (right) short nozzle. Colors represent configurations; without mixer (black), mixer with 12 lobes (red), mixer with 16 lobes (green).

In the following the mixer has been modelled as chevrons located at the exit of the equivalent single

stream nozzle using the suppressed-to-unsuppressed wetted perimeter ratio PR_I [6], where the required input (various perimeters and diameters) was extracted from the mixer CAD geometry. Figure 19 shows the simulated spectra as dashed lines, resulting from the chevrons analogy modelling. It can be observed that the predicted mixer effect trend now shows an improved agreement with the experimental results.

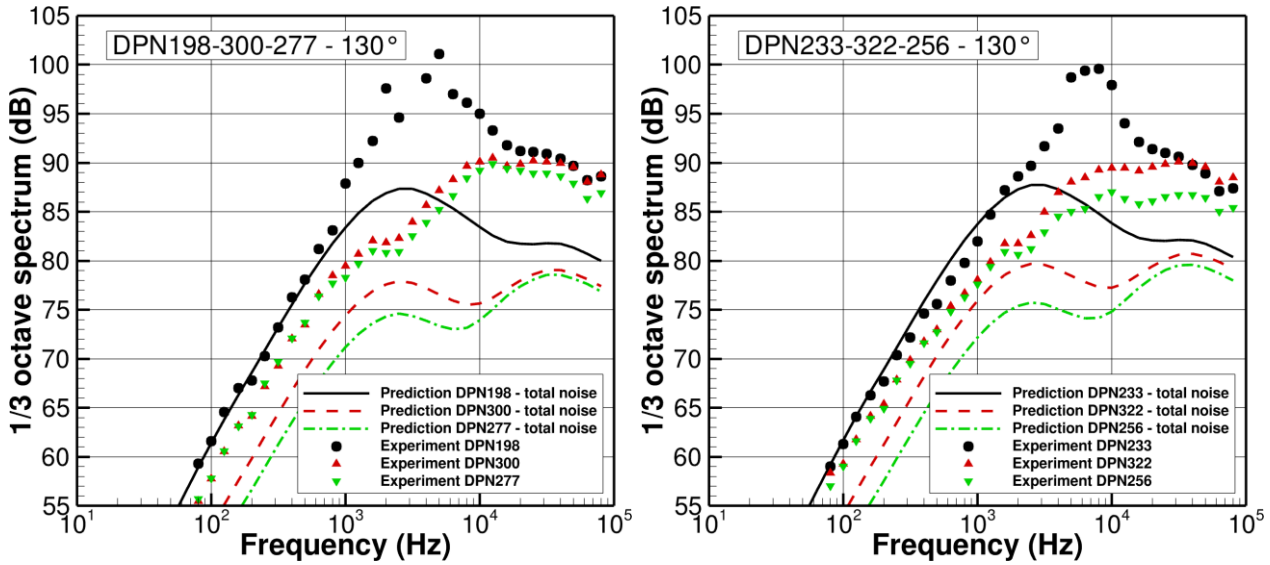

Figure 19 – Comparison between measured and predicted jet noise: effect of mixer for (left) long nozzle and (right) short nozzle. Colors represent configurations; without mixer (black), mixer with 12 lobes (red), mixer with 16 lobes (green). Simulated data with chevrons modelling.

5.3 Effect of nozzle length

Recalling that for mixed-flow nozzles (i.e. inner- and outer stream have different flow properties), the modelling has been performed by assuming a single stream jet with perfect mixing, the effect of nozzle length for configurations with external plug also has been simulated in this way. Figure 20 shows a comparison between test and prediction results, each for a short and long nozzle without mixer. The flow can be considered as high subsonic conventional profile dual stream (NPR_{inner}=1.8 and NPR_{outer}=1.1). Although the low-frequency noise shows good agreement, the mid-to-high frequency noise is underpredicted. This is partly due to the appearance of tones in the experimental setup.

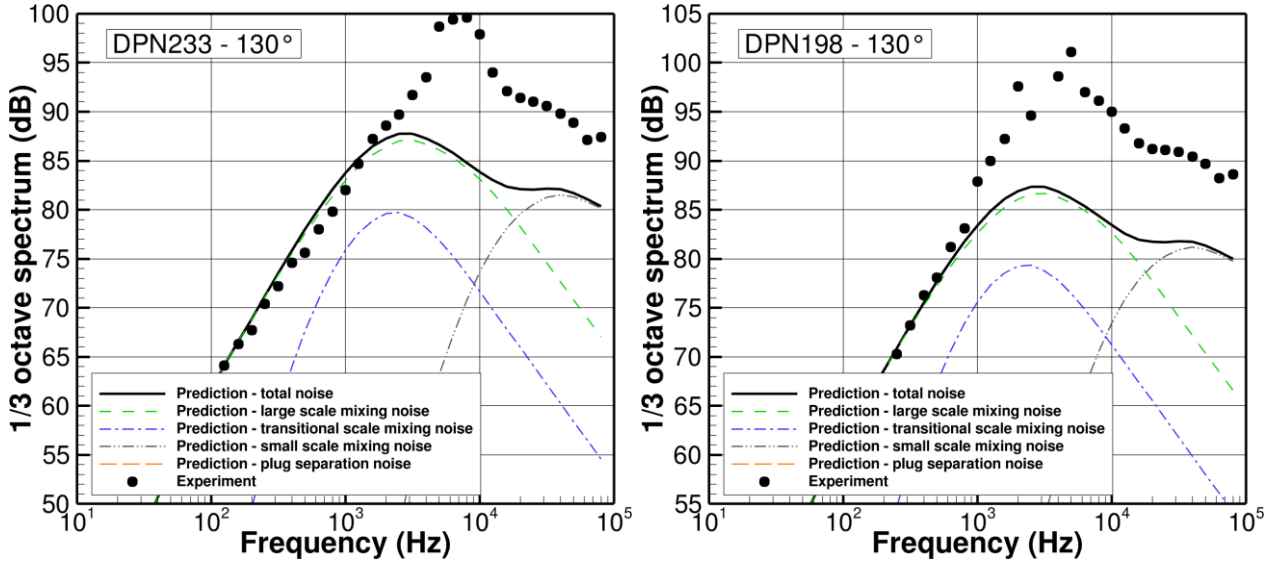

Figure 20 – Comparison between measured and predicted jet noise: effect of nozzle length without mixer, (left) short nozzle, (right) long nozzle.

Figure 21 shows the effect of nozzle length for experiment and prediction separately. The prediction does not show a significant effect, which might be found in the experimental data as well if the tones would be omitted.

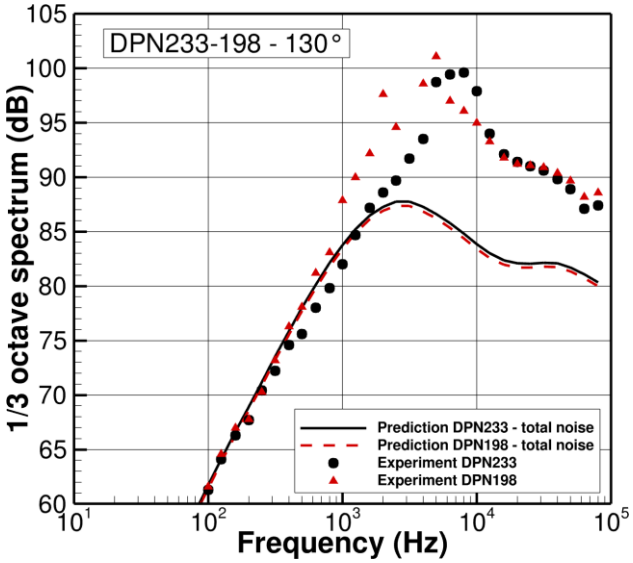

Figure 21 – Comparison between measured and predicted jet noise: effect of nozzle length without mixer. Black represents a short nozzle and red a long nozzle.

Figure 22 shows a comparison between test and prediction results, each for a short and long nozzle with the 16 lobed mixer (without chevrons modelling for the simulated data). The low-to-mid frequency noise is predicted well, but the high frequency noise is underpredicted. Figure 23 shows the effect of nozzle length for experiment and prediction separately. Although the presence of a mixer enforces the flow mixing better than the confluent nozzle, the predicted effect of nozzle length does not agree well with the experimental spectra. Where the experiment showed for the high frequency broadband noise an increased level, the prediction showed a minor decreased level.

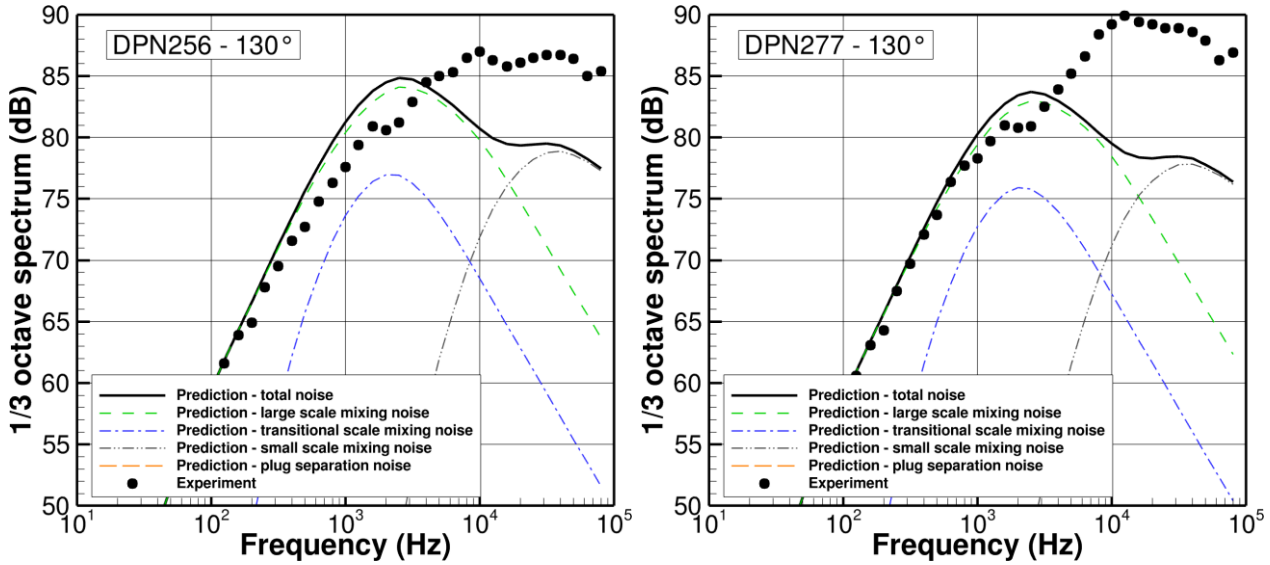

Figure 22 – Comparison between measured and predicted jet noise: effect of nozzle length with 16 lobes mixer, (left) short nozzle, (right) long nozzle.

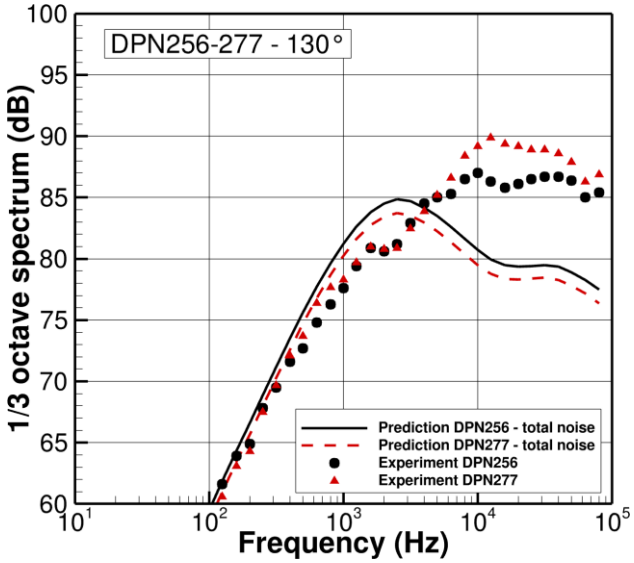

Figure 23 – Comparison between measured and predicted jet noise: effect of nozzle length with 16 lobes mixer. Black represents a short nozzle and red a long nozzle.

5.4 High-fidelity simulation

A RANS-based approach described in Ref. [21] has been applied to the nozzle configurations without mixer and with two different lengths of the external duct. The approach is based on the acoustic analogy models of Morris & Boluriaan [17] and Miller & Morris [18] - [20]. Starting from the in-homogeneous Linearized Euler Equation (LEE) the acoustic spectral density is expressed as a convolution integral among the Green's functions of the homogeneous LEE and the two-point cross correlation of equivalent sources. The latter ones consider both the contribution of the turbulent mixing noise and the shock associated noise. The equivalent sources are correlated to the turbulent length scales estimated from the RANS simulations and the calibration constants of the model have been previously tuned on single stream jets.

The dual stream nozzle has been modelled as an axial-symmetric domain which extends 100 diameters downstream of the jet and 50 diameters in cross-wise direction. A structured mesh was generated guaranteeing a fully resolved turbulent boundary layer near the nozzle walls as well as the grid has been properly refined in the plume and in the shear layer regions. To replicate the experimental setting, the free-stream boundary conditions have been set to the ambient pressure and temperature (p_∞ = 101000 Pa and T_∞ = 295 K for the long duct and p_∞ = 100000 Pa and T_∞ = 294 K for the short duct). The nozzle boundary conditions have been set to nozzle pressure ratio NPR_{inner} = 1.80 and NPR_{outer} = 1.11 for both nozzle configurations.

The steady RANS solution has been achieved by using the commercial software Ansys-Fluent adopting the Menter SST model for the Reynolds stress tensor. The mean-flow solution and the turbulent quantities have been finally used to feed the acoustic model.

Figure 24 (left) shows that the Mach number is fairly subsonic reaching values around 0.95 at the exit of the nozzle, with a spot of Mach equal to 1 for the short duct. However, the presence of the plug curvature decelerates the flow as it approaches to the plug tip, generating a pressure jump at its sharp tip. Since shock-associated noise is generated in regions where the product of the strength of the shock cells and the turbulent shear layer is significant, thus likely proportional to |p - p_∞|K/p_∞ where K is the turbulent kinetic energy, a shock-associated noise contribution is predicted by the RANS simulation, see Figure 24 (right).

Figure 25 depicts the position of the noise source regions in the jet plume, showing the shock associated noise is due to the pressure jump generated by the plug whereas the mixing component is related to the turbulent kinetic energy in the jet shear layer.

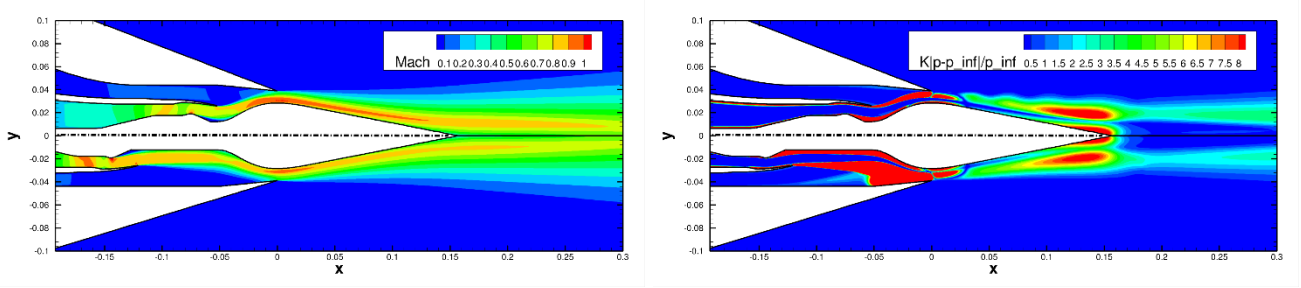

Figure 24 – Contours of jet-flow: solution for the short duct nozzle on the top and the long duct on the bottom; Mach number (left) and relative pressure $K|p-p_\infty|/p_\infty$ (right).

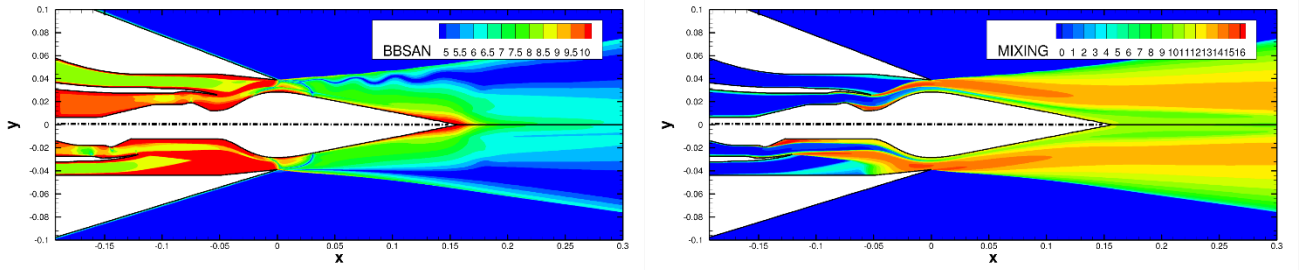

Figure 25 – Contours of jet-noise sources in logarithmic scale: solution for the short duct nozzle on the top and the long duct on the bottom; shock-associated noise (left) and turbulent mixing noise (right).

Figure 26 and Figure 27 show a comparison between experimental and RANS-based prediction results at two polar angles, each for a short and long nozzle without mixer. More specifically, Figure 26 (left) and Figure 27 (left) represent the noise sources contribution to the one-third octave band spectrum for the long duct, showing that the predicted shock contribution allows to explain the experimental spectrum peak around 5 kHz, even though the mixing contribution seems to overpredict the lower frequency region with respect to the experimental spectrum. Figure 26 (right) and Figure 27 (right) show the total noise for the long and short nozzle, yielding a fairly good agreement with the experimental data.

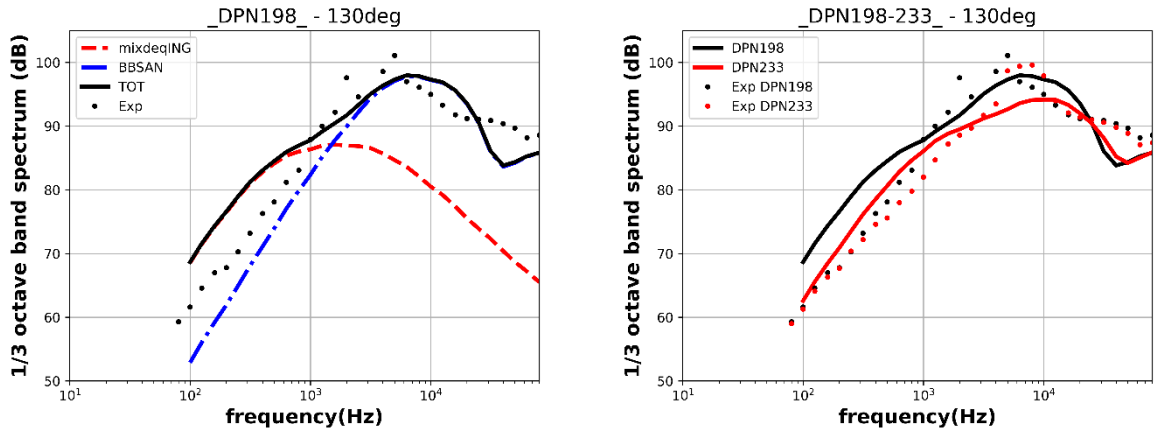

Figure 26 – Comparison between measured and RANS-based predicted jet noise at polar angle 130 deg. On the left, contribution of noise sources for the long nozzle, (red) mixing and (blue) shock-associated. On the right, effect of nozzle length without mixer, (red) short nozzle, (black) long nozzle.

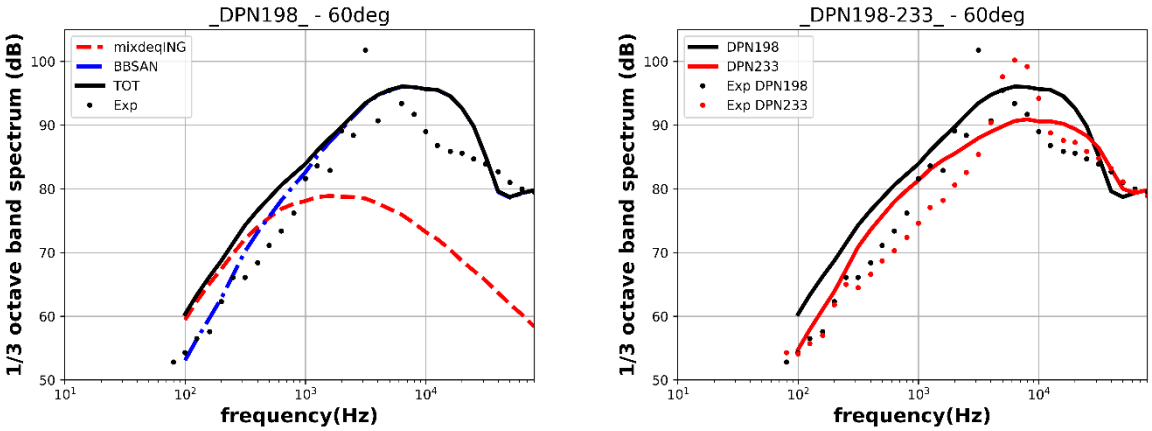

Figure 27 – Comparison between measured and RANS-based predicted jet noise at polar angle 60 deg. On the left, contribution of noise sources for the long nozzle, (red) mixing and (blue) shock-associated. On the right, effect of nozzle length without mixer, (red) short nozzle, (black) long nozzle.

6. Conclusions

Within the EU-Project SENECA a small-scale acoustic jet noise test has been designed, performed and experimental data have been processed and analyzed. The test model can be expected to be representative to an engine nozzle of future commercial supersonic aircraft. The present paper presents an overview of the model design, test and measurement setup, test program and experimental results. The experimental results allow trend effect analysis. The following trends have been observed and are compared to the scarcely available literature in the public domain.

Effect of mixer and lobes:

- A mixer can reduce broadband jet noise in a broad frequency range and can suppress tones additionally.
- Increasing the number of lobes for a short nozzle can reduce the noise further in the middle and high frequency range.
- A mixer changes the directivity characteristic for high emission angles, where the number of lobes is not affecting the directivity.

These observations are qualitatively in line with available literature. Mengle & Dalton [15] showed that a mixer reduces low frequency noise but can increase mid-to-high frequency noise. Bridges et al. showed that a mixer yields SPL reduction in a broad frequency range and suppresses peaks [8]. The effect of a mixer was found not to be significant for fully mixed flow [8]. Both Garrison et al. [12] and Bridges & Wernet [13] showed that when a mixer reduces the maximum noise level it can also generate high-frequency noise. Mengle & Dalton [15] also found that increasing the number of lobes decreases the overall noise (by reduction of mid-to-high frequency noise at static conditions). Krasheninnikov et al. [14] observed that increasing the number of lobes only has a marginal noise reduction effect.

Effect of nozzle length:

- Increasing the nozzle length for unmixed flows i) reduces the noise in the middle frequency range, and ii) can generate tones in a broad frequency range.
- Increasing the nozzle length for mixed flows can result into increased noise levels in the high frequency range.
- For unmixed flows increasing the nozzle length changes the directivity only for the higher radiation angles. For mixed flows increasing the nozzle length amplifies the directivity pattern to a slightly increased maximum OASPL.

A comparison of these observations with available literature yields a less clear image. Bridges et al. [8] report a frequency shift of a spectral hump at high frequency, with higher frequency elevated levels for a short duct. This is not observed in the present study. Additionally, increasing nozzle length is shown to yield increased levels in the low-frequency range and decreased levels in the

high-frequency range [8]. It is currently not clear if this can be compared to the similarly observed trend of the unmixed flow condition of the present study. Mengle & Dalton [15] already observed for lobed mixers without external plug that increasing the nozzle length does not necessarily reduces the mid-to-high frequency noise.

Finally, a comparison assessment of the noise spectra between experimental data and jet noise predictions has been performed. Semi-empirical predictions for a coannular nozzle i) suggest that the found high-frequency bump in the experimental data can be explained by plug separation noise, and ii) emphasize the importance of prediction assumption of the jet expanding under ambient static pressure. As there are no publicly available semi-empirical prediction methods for internally mixed exhaust flows, the respective modelling has been performed by assuming a single stream jet with perfect mixing. In general, an underprediction of the mid-to-high frequency noise can be observed. For the prediction of mixer trend effects, using a chevrons analogy provides good agreement with the experimental results without requesting additional experimental data. Prediction results of nozzle length trend effects do not agree well with the experimental spectra. High-fidelity predictions based on computational fluid dynamics for nozzles without mixer show better agreement with the experimental noise spectra in the mid-to-high frequency range and could be considered for improved understanding of internally mixed exhaust flows. On the other hand they need to be validated by large experimental databases.

7. Contact Author Email Address

Mail to: remco.habing@nlr.nl

8. Funding

This research was funded by the European Union's Horizon 2020 research and innovation programme under grant agreement No. 101006742, project SENECA ((LTO) Noise and Emissions of Supersonic Aircraft).

9. Acknowledgments

The authors would like to thank Dr. James Bridges from NASA Glenn RC for providing STEP files of the Plug20 nozzles parts. The authors also would like to thank Mr. Gert-Jan van Toly from NLR for the design and manufacturing coordination of the model parts.

10. Copyright Statement

11. References

[1] Petrosino F and Barbarino M, Comparison of analytical semi-empirical model for jet noise prediction. *33rd Congress of ICAS*, 2022.

[2] Jaron R, Gräbert M, Habing R, Van der Meulen M, Huet M, LeGriffon I, Petrosino F, Barbarino M, Lefarth K and Zaporozhets O, Jet Noise Prediction Benchmark for Landing and Takeoff Noise of Supersonic Aircraft. *InterNoise*, 2023.

[3] Bridges J and Wernet M, Noise of Internally Mixed Exhaust Systems With External Plug For Supersonic Transport Applications. *AIAA Aviation Forum*, AIAA paper 2021-2218, 2021.

[4] James R. Stone, Donald E. Groesbeck, and Charles L. Zola. Conventional profile coaxial jet noise prediction. *AIAA Journal*, 21(3):336–342, 1983.

[5] James Stone, Charles Zola, and Bruce Clark. An improved model for conventional and inverted-velocityprofile coannular jet noise. *37th Aerospace Sciences Meeting and Exhibit*, AIAA paper 99-0078, 1999.

[6] JR Stone, EA Krejsa, BJ Clark and JJ Berton. Jet noise modeling for suppressed and unsuppressed aircraft in simulated flight. *NASA Technical Memorandum*, NASA-TM-2009-215524, 2009.

[7] Zaman Kh and Heberling B, A Study of Flow and Noise from Supersonic Plug Nozzles. *AIAA Aviation Forum*, AIAA paper 2021-2304, 2021.

[8] Bridges J, Podboy G and Wernet M, Plug20 Test Report. *NASA* TM-20210010291, 2021.

[9] Viswanathan K, Distribution of noise sources in heated and cold jets: are they different?. *Int. J. Aeroacoustics*, 9(4-5), 589-625, 2010.

[10] Viswanathan K, True farfield for dual-stream jet noise measurements. *AIAA J.*, 49(2), 443-447, 2011.

[11] Lammers K, Habing R, Grossir G and Schram Ch, Jet noise of an airframe-integrated dual-mode nozzle propulsion system during take-off and landing. *2nd Int. Conf. on High-Speed Vehicle Science Techn.*, *HiSST*-2022-315,2022.

[12] Garrison L, Dalton W, Lyrintzis A and Blaisdell G, On the Development of Semi-Empirical Noise Models for the Prediction of the Noise from Jets with Forced Mixers. *AIAA paper 2004-2898*, 2004.

[13] Bridges J and Wernet M, Cross-Stream PIV Measurements of Jets With Internal Lobed Mixers. *AIAA Aviation Forum*, AIAA paper 2004-2896, 2004.

[14] Krasheninnikov S, Mironov K, Pavlyukov E, Shenkin A and Zhitenev V, Mixer-ejector nozzles: acoustic and thrust characteristics. *Int. J. aeroacoustics,* volume 4, no. 3&4, p. 267 – 288, 2005.

[15] Mengle VG and Dalton WN, Lobed mixer design for noise suppression; Acoustic and aerodynamic test data analysis, *NASA/CR-2002-210823/VOL1*, 2002.

[16] Banks W, Parametric Mixer Design Methods for Acoustic Explorations of Internally Mixed Nozzles, *NASA Acoustics Technical Working Group,* 19 October 2021.

[17] Morris, P., and Boluriaan, S., "The Prediction of Jet Noise from CFD Data," *10th AIAA/CEAS Aeroacoustics Conference*, 2012. https://doi.org/10.2514/6.2004-2977, URL https://arc.aiaa.org/doi/abs/10.2514/6.2004-2977.

[18] Miller, S. A. E., "Toward a Comprehensive Model of Jet Noise Using an Acoustic Analogy," *AIAA Journal*, Vol. 52, No. 10, 2014, pp. 2143–2164. https://doi.org/10.2514/1.J052809, URL https://doi.org/10.2514/1.J052809.

[19] Morris, P. J., and Miller, S. A. E., "Prediction of Broadband Shock-Associated Noise Using Reynolds-Averaged Navier-Stokes Computational Fluid Dynamics," *AIAA Journal*, Vol. 48, No. 12, 2010, pp. 2931–2944. https://doi.org/10.2514/1.J050560, URL https://doi.org/10.2514/1.J050560.

[20] Miller, S. A. E., and Morris, P. J., "The Prediction of Broadband Shock-Associated Noise Including Propagation Effects," *International Journal of Aeroacoustics*, Vol. 11, No. 7-8, 2012, pp. 755–781. https://doi.org/10.1260/1475-472X.11.7-8.755, URL https://doi.org/10.1260/1475-472X.11.7-8.755.

[21] Barbarino, M., Petrosino, F., Piccirillo, G., Glorioso, A., Viola, N., "A RANS-based Acoustic Analogy approach for Jet-Noise assessment of next-generation Supersonic Aircraft", *In proceedings of the 30th AIAA/CEAS Aeroacoustics Conference*, 4 -7 June, 2024.